Pre-neutron-emission mass distributions for reaction ^{238}U(n, f) up to 60 MeV *

SUN Xiao-Jun(孙小军)[1;1)] YU Cheng-Gang(余呈刚)[2] WANG Ning(王宁)[1]
YANG Yong-Xu(杨永栩)[1] PAN Cheng-Hua(潘成华)[1]

[1] College of Physical Science and Technology, Guangxi Normal University, Guilin 541004, China
[2] Shanghai Institute of Applied Physics, Chinese Academy of Sciences, Shanghai 201800, China

Abstract: The pre-neutron-emission mass distributions for reaction ^{238}U(n, f) up to 60 MeV are systematically studied with an empirical fission potential model. The energy dependence of the peaks and valleys of the pre-neutron-emission mass distributions is described by an exponential form based on the newly measured data. The energy dependence of evaporation neutrons before scission is also considered, which plays a crucial role in the reasonable description of the mass distributions. The measured data of the pre-neutron-emission mass distributions for reaction ^{238}U(n, f) are reasonably well reproduced up to 60 MeV. The mass distributions at unmeasured energies are also predicted using this approach.

Key words: reaction ^{238}U(n, f), pre-neutron-emission mass distribution, evaporation neutron, fission potential

PACS: 24.75.+i **DOI:** 10.1088/1674-1137/39/1/014102

1 Introduction

Since the discovery of neutron-induced fission of uranium in 1938 [1], the neutron-induced fission has become the subject of both theoretical and experimental studies. In the past, tremendous efforts have been focused on the low-energy actinide fission because of the particular importance for nuclear energy applications. Nowadays, there is an increasing interest in studying neutron-induced fission of actinides at intermediate energies. It is motivated by nuclear data needs for new applications such as accelerator-driven systems, thorium-based fuel cycles, and the next generation of exotic beam facilities. The pre-neutron-emission mass distribution is one of the most important quantities for neutron-induced fission. Its precise description is of great importance in both understanding the fission mechanism and the practical application. In addition, ^{238}U is one of the most important actinides, and its disposal in spent fuel (^{238}U is up to 95%) is an important feature of the utilization in the nuclear power field.

Although one can qualitatively describe the nuclear fission process as a deformation of a single nucleus, the exact understanding of the fission process or quantitative prediction of the pre-neutron-emission fragment mass distributions or product yields are still very elusive for the existing theories and models [2]. An international working group has studied the overall problem and recommended the assembly of the required nuclear data (including fission products) at intermediate incident neutron energies up to 150 MeV [3]. Compared with low-energy fission, the modeling of neutron-induced fission at intermediate energies is severely complicated by the fact that fission follows pre-equilibrium particle emission and competes with neutron evaporation [4].

Several important theories and models [2, 5–17] have been developed for understanding the fission mechanism or quantitatively calculating the fragment mass distributions or fission product yields. These models are mainly focused on the dynamical processes. The systematic approaches, which consist of three to seven Gaussian functions, have been developed for quantitatively predicting the fragment mass distributions or product yields [18–21].

A combination method based on the driving potential from the Skyrme energy-density functional [22, 23] and the phenomenological fission potential was proposed in our previous work [24], and the experimental pre-neutron-emission mass distributions of neutron-induced actinide fission at low energies have been reasonably well reproduced. The present study is an extension of this combination method for reaction ^{238}U(n, f) at incident

Received 24 March 2014
* Supported by Guangxi University Science and Technology Research Projects (2013ZD007), Guangxi Natural Science Foundation (2012GXNSFAA053008), and National Natural Science Foundation of China (11265004)
1) E-mail: sxj0212@gxnu.edu.cn

energies up to 60 MeV. This paper is organized as follows. In Section 2, the combination method and the potential parameters are introduced in detail. In Section 3, the comparisons of the calculated results and the measured data for reaction ^{238}U(n, f) are presented and analyzed. A simple summary is also given in the this section.

2 The combination method and the potential parameters

The sequential products of neutron-induced binary fission are elaborated in Refs. [24, 25]. A combination method for calculating the pre-neutron-emission mass distributions of neutron-induced actinide fission at low energies was proposed in our previous work [24]. In this model, the pre-neutron-emission mass distributions are described as

$$P(A)=C\exp[-U(A)], \tag{1}$$

where C is the normalization constant, and the variable A denotes the mass number of the primary fragment. The phenomenological fission potential $U(A)$ is described by three harmonic-oscillator functions, i.e.

$$U(A)=\begin{cases} u_1(A-A_1)^2 & A\leqslant a, \\ -u_0(A-A_0)^2+R & a\leqslant A\leqslant b, \\ u_2(A-A_2)^2 & A\geqslant b, \end{cases} \tag{2}$$

where A_1 and A_2 are the positions of the light and heavy fragment peaks of the pre-neutron-emission mass distributions, respectively. A_0 denotes the corresponding position for symmetric fission. The fission potential parameters u_1, u_0, u_2, a, b and R, which are the functions of A_0, A_1 and A_2, were uniquely derived as Eq. (6)–Eq. (9) in our previous paper [24].

Particular attention should be paid to these parameters which are closely related to the evaporation neutrons before scission at different incident energies. For reaction ^{238}U(n, f) at low incident energies ($E_{\rm n}\leqslant 6.5$ MeV), the positions A_1 and A_2 are obtained from the nucleus-nucleus driving potential of the fissile nucleus ^{239}U [22, 23]. With the incident neutron energy increasing, the excitation energy of the compound nucleus will become higher, and a few neutrons will be evaporated before scission. The number of evaporation neutrons can be derived from the corresponding multi-chance fission cross sections. Therefore, the fission cross sections of reaction ^{238}U(n, f) have been investigated as shown in Fig. 1. The scattering dots denote the experimental data derived from Refs. [26–28], and the solid curve denotes the evaluated results of ENDF/B-Ⅶ.1, which are recommended as the standard cross sections. The dash, dot and dash dot curves denote the (n, nf), (n, 2nf) and (n, 3nf) fission cross sections evaluated by ENDF/B-Ⅶ.1, respectively. The perpendicular dash lines label the incident energy regions corresponding to the different multi-chance fission channels such as (n, f), (n, nf), (n, 2nf) and (n, 3nf) in this paper, respectively. From Fig. 1, one establishes that the number $\tilde{n}(E_{\rm n})$ of evaporation neutrons before scission can be roughly expressed as follows

$$\tilde{n}(E_{\rm n})=\begin{cases} 0, & E_{\rm th}\leqslant E_{\rm n}\leqslant 6.5\ \text{MeV}, \\ 1, & 6.5\ \text{MeV}<E_{\rm n}\leqslant 14.5\ \text{MeV}, \\ 2, & 14.5\ \text{MeV}<E_{\rm n}\leqslant 21.5\ \text{MeV}, \\ 3 & 21.5\ \text{MeV}<E_{\rm n}\leqslant 60\ \text{MeV}. \end{cases} \tag{3}$$

where $E_{\rm th}$ is the threshold energy for ^{238}U(n, f) reaction. Eq. (3) is consistent with the result at low incident energies as shown in Ref. [24]. It is worth mentioning that the neutron number over 3 is not observed by both experiments and certified by theories before scission with increasing incident energies (even up to 100 MeV) for reaction ^{238}U(n, f). The small insert in Fig. 1 shows that the total fission cross sections attain a maximum of about 40 MeV, and are smaller with increasing incident energies. It implies that the reaction channels, such as (n, 4nf) and (n, 5nf), will not contribute to the total fission probability. This phenomenon is caused by the competition involving all reaction channels for neutron-induced ^{238}U reaction. Thus in this paper, it is established that

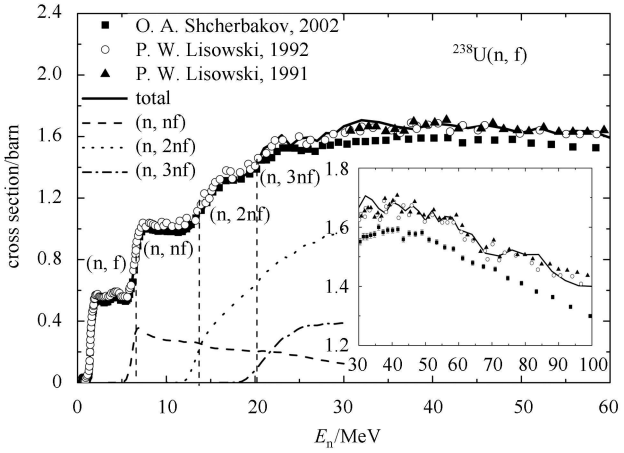

Fig. 1. The fission cross section of reaction ^{238}U(n, f) for incident neutron energies from threshold energy to 60 MeV. The experimental data are obtained from Refs. [26] (squares), [27] (circles) and [28] (triangles), respectively. The solid, dash, dot and dash dot curves denote the total, (n, nf), (n, 2nf) and (n, 3nf) fission cross sections evaluated by ENDF/B-Ⅶ.1, respectively. The perpendicular dash lines label the incident energy regions corresponding to the different multi-chance fission channels such as (n, f), (n, nf), (n, 2nf) and (n, 3nf) in this paper, respectively. The insert shows the experimental and evaluated data from 30 to 100 MeV.

there are no other channels, such as (n, 4nf), (n, 5nf), et al.

It is assumed that a compound nucleus $A_{\rm CN}$ after evaporating neutrons $\tilde{n}(E_{\rm n})$ separates into a pair of fragments in the fission process, so the mass number of the fissile nucleus is $A_{\rm FN}=A_{\rm CN}-\tilde{n}(E_{\rm n})$ in different incident energy regions. For reaction ^{238}U(n, f), the fissile nuclei are ^{239}U, ^{238}U, ^{237}U and ^{236}U, respectively, in different incident energy regions as listed in Eq. (3) and shown in Fig. 1. Based on the nucleus-nucleus potential with the Skyrme energy-density functional [22, 23], the driving potentials of these fissile systems are studied considering the deformations of fragments. One sees that these driving potentials generally show a valley at $A\sim140$ for the mass distributions of heavy fragments, as elaborated in Fig. 1 in Ref. [24]. It should be noted that the driving potentials are only derived from the ground state or low excited energies of the fragments. However, the fissile nuclei still hold highly excited energies after evaporating neutrons in different incident energy regions. So the position A_2 of the heavy fragment peaks, as well as A_1 of the light fragment peaks and A_0 of the symmetrical fission, should be modified as

$$\begin{cases} A_2=A_2^{\rm g.s.}-\tilde{n}(E_{\rm n}), \\ A_1=A_{\rm FN}-A_2, \\ A_0=A_{\rm FN}/2, \end{cases} \tag{4}$$

where $A_2^{\rm g.s.}\approx140$ denotes the lowest position of the driving potential derived from the ground state of the fragments. The results of Eqs. (3) and (4) agree exactly with the positions of the maximal mass distributions of the heavy fragments measured by the quasi-monoenergetic neutrons beam from 10 MeV up to 60 MeV [4, 29] as listed in Table 1. For comparison, the results of TALYS code [17] are also listed in this table.

Table 1. The positions (A_1,A_2) for the mass number of the light and heavy fragment mass distributions for reaction ^{238}U(n, f) in different incident energy regions.

$E_{\rm n}$/MeV	Exp. [31]	TALYS [17]	this work
9–11	(99, 138)	(99, 139)	(99, 139)
16–18	(99, 138)	(99, 138)	(99, 138)
24–26	(98, 138)	(99, 138)	(99, 137)
33	(99, 137)	(98, 137)	(99, 137)
45	(99, 137)	(98, 137)	(99, 137)
60	(99, 136)	(98, 136)	(99, 137)

Based on the monoenergetic experimental data [30] and the quasi-monoenergetic experimental data [4, 29], the heights $P(A_0)$ and $P(A_1)$ of the valleys and peaks of the pre-neutron-emission mass distributions have been fitted as the functions of incident neutron energies. For reaction ^{238}U(n, f) up to 60 MeV, the energy dependence of $P(A_1)$ and $P(A_0)$ is written as

$$\begin{aligned} P(A_1)&=3.850+2.600{\rm e}^{-0.040E_{\rm n}}, \\ P(A_0)&=0.044+4.581{\rm e}^{-32.465/E_{\rm n}}. \end{aligned} \tag{5}$$

The results of the measurement, including the white neutron beam [31], monoenergetic neutron [30] and the quasi-monoenergetic neutron [4, 29], and the calculation are shown in Fig. 2. So the parameter R in Eq. (2) can be derived easily through Eq. (6) as shown below

$$R=\ln\frac{P(A_1)}{P(A_0)}. \tag{6}$$

Furthermore, Eq. (5) approximatively equals the results of Ref. [24] at low incident energy ($E_{\rm n}\leqslant6.5$ MeV). One can see that the values of $P(A_1)$ and $P(A_0)$ exponentially change with the incident energies in general, which could provide some useful information at unmeasured energies.

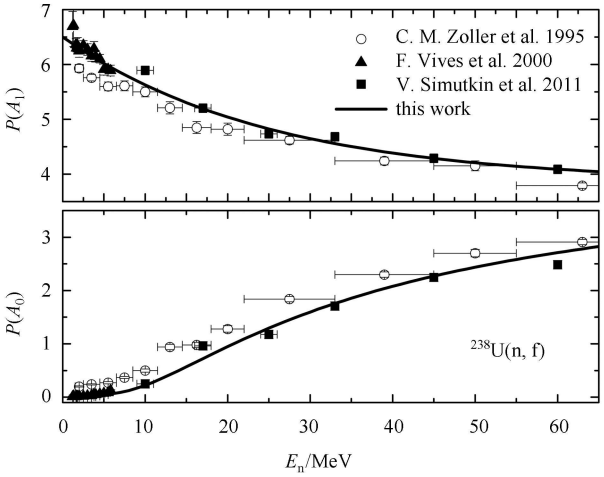

Fig. 2. Peak $P(A_1)$ and valley $P(A_0)$ of the pre-neutron-emission mass distributions for reaction ^{238}U(n, f) as a function of incident neutron energy. The experimental data are derived from the white neutron beam (circles) [31], monoenergetic neutron (triangles) [30] and the quasi-monoenergetic neutron (squares) [4, 29]. The solid lines denote the results of this work.

3 Results and analysis

In this work, the evaporation neutrons $\tilde{n}(E_{\rm n})$ in different incident energy regions are derived from the fission cross sections in multi-chance fission channels as shown in Fig. 1. In terms of the evaporation neutrons $\tilde{n}(E_{\rm n})$, the positions A_2 of the heavy fragment peaks of the pre-neutron-emission mass distributions are determined. So the positions A_1 of the light fragment peaks can be also obtained easily. Combining the heights $P(A_0)$ and $P(A_1)$ of the valleys and peaks of the pre-neutron-emission mass distributions as shown in Fig. 2, the parameter R is also obtained in terms of Eq. (6). So the pre-neutron-emission

mass distributions can be calculated using Eqs. (1) and (2) up to 60 MeV, as shown in Fig. 3 and Fig. 4. Fig. 3 shows the pre-neutron-emission mass distributions of reaction ^{238}U(n, f) at low incident energies from 1.3 MeV to 5.5 MeV, and one can see that these results agree with the previous results of Ref. [24]. Fig. 4 shows the calculated results up to 60 MeV. In this figure, the scattered symbols denote the experimental data, which are taken from Refs. [4, 29] (squares, measured by the quasi-monoenergetic neutron) and from Ref. [31] (circles, measured by the white neutron beam), respectively. The solid curves denote the calculated results in this work. The dash curves denote the results calculated by TALYS code [17]. One can see that the experimental data of reaction ^{238}U(n, f) can be reproduced well from the threshold energy up to 60 MeV. It indicates that the method combining the driving potential with the phenomenological fission potential is reasonable to describe the pre-neutron-emission mass distributions of reaction ^{238}U(n, f) up to 60 MeV.

To extend this method, the pre-neutron-emission mass distributions at unmeasured energies are also predicted up to 100 MeV shown in Fig. 5. One can see that several distinct characters of the pre-neutron-emission mass distributions can be reasonably reproduced: (1) the double bump shape; (2) the increase of the valley heights, as well as the decrease of the peak heights, with the incident energy increasing; (3) the position A_2 of the heavy fragment peak locates roughly 140 at low energies, and gradually decreases because of the evaporation neutrons before scission at E_n >6.5 MeV. Contrarily, the position A_1 of the light fragment peak always locates roughly 99 as mentioned in Ref. [8]. This implies that the combination method in this paper can provide some additionally useful information for the intermediate energies of neutron induced actinides fission.

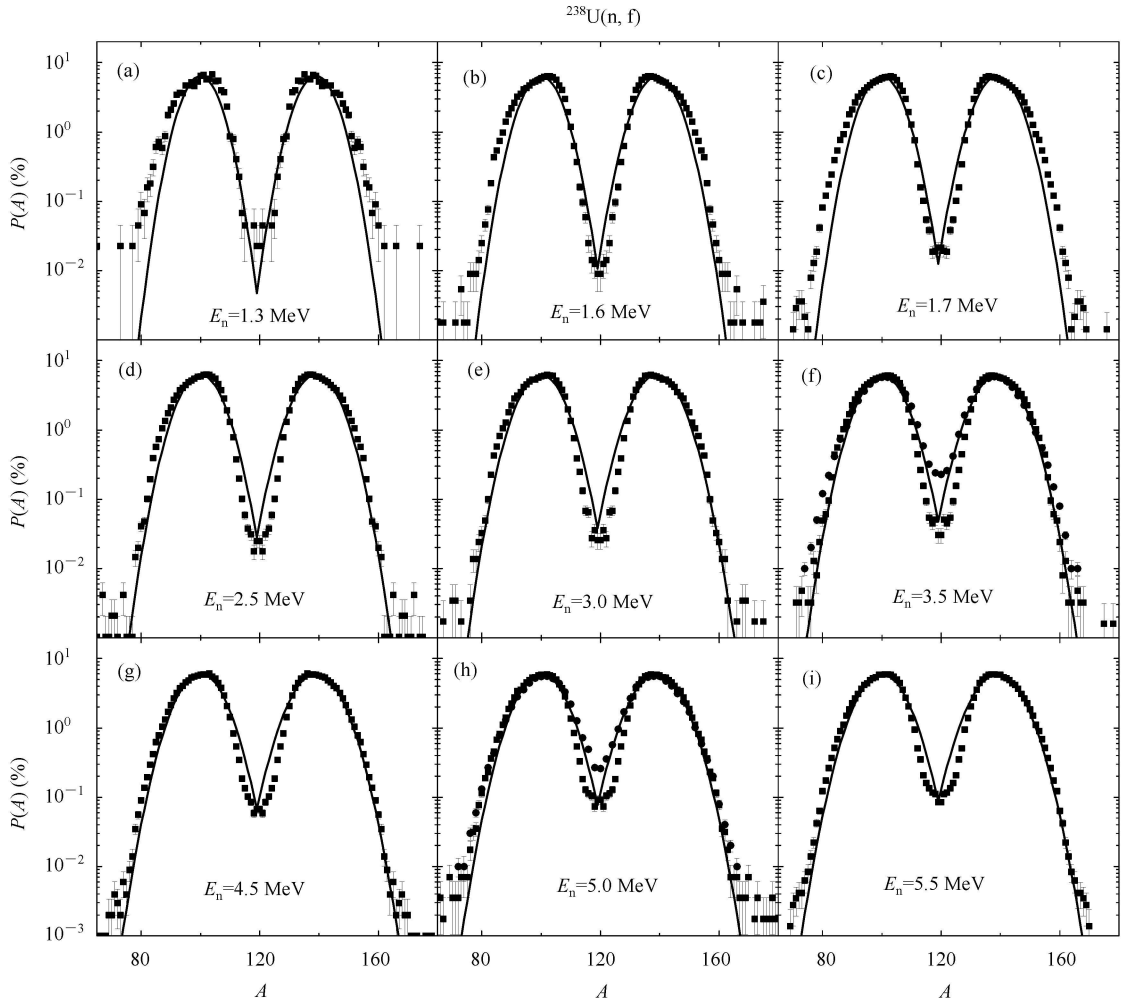

Fig. 3. Pre-neutron-emission mass distributions at incident energies from 1.3 to 5.5 MeV for reaction ^{238}U(n, f). The scattered symbols denote the experimental data, which are taken from Ref. [30] (squares, measured by the monoenergetic neutron) and from Ref. [31] (circles, measured by the white neutron beam), respectively.

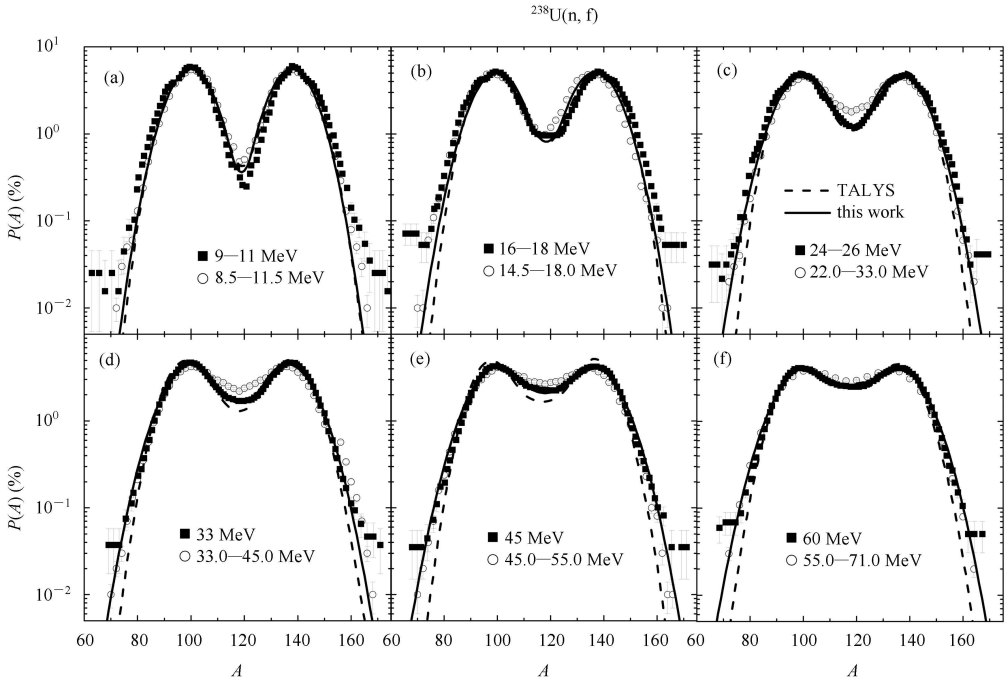

Fig. 4. Pre-neutron-emission mass distributions at incident energies from 10 to 60 MeV for reaction ^{238}U(n, f). The scattered symbols denote the experimental data, which are taken from Refs. [4, 29] (squares, measured by the quasi-monoenergetic neutron) and from Ref. [31] (circles, measured by the white neutron beam), respectively. The dash and solid curves denote the calculated results of TALYS code [17] and in this work, respectively.

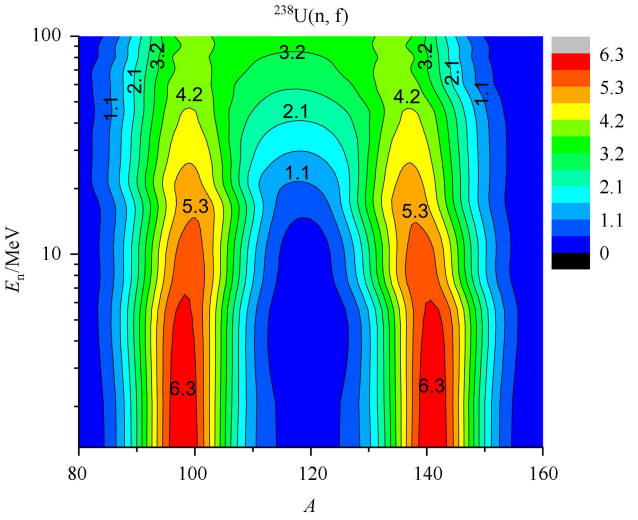

Fig. 5. (color online) The calculated pre-neutron-emission mass distributions (%) at incident energies from the threshold energy up to 100 MeV for reaction ^{238}U(n, f) involved the fragment mass number A and the incident energy $E_{\rm n}$.

4 Summary

In this paper, the pre-neutron-emission mass distributions for reaction ^{238}U(n, f) from the threshold energy up to 60 MeV are well reproduced using an empirical fission potential, whose potential parameters are uniquely derived from the existing experimental data. The energy dependence of evaporation neutrons before scission is also considered, which plays a crucial role in the reasonable description of the mass distributions. The energy dependence of the peaks and valleys of the pre-neutron-emission mass distributions is described by the exponential expressions based on the newly measured data. The double-humped shapes of the measured pre-neutron-emission mass distributions are reasonably well reproduced from low incident energies to intermediate incident energies. The pre-neutron-emission mass distributions at unmeasured energies are also predicted up to 100 MeV using this method.

In addition, we compare the calculated results using the previous method and the parameters [24], and the results of this work are slightly improved at low incident energies. We have also compared the experimental data at intermediate energies with the model calculations of TALYS, and one can see that the results of this work reproduce the experimental data better. Furthermore, a more microscopic description of the potential parameters should be further investigated. The study of these aspects is underway.

We wish to thank our colleagues Ou L, Liu M and an anonymous referee for some valuable suggestions.

References

1 Hahn O, Strassmann F. Naturwissenschaften, 1939, **27**: 11–15
2 Randrup J, Möller P. Phys. Rev. Lett., 2011, **106**: 132503
3 Lammer M. Proc. Fission Product Yields: Minor Actinides up to 150 MeV. Ed. Lammer M. Vienna: IAEA, 2008. 1
4 Ryzhov I V, Yavshits S G, Tutin G A et al. Phys. Rev. C, 2011, **83**: 054603
5 Goutte H, Berger J F, Casoli P et al. Phys. Rev. C, 2005, **71**: 024316
6 Vanin D V, Kosenko G I, Adeev G D. Phys. Rev. C, 1999, **59**: 2114–2121
7 Karpov A V, Nadtochy P N, Vanin D V et al. Phys. Rev. C, 2001, **63**: 054610
8 HU J M. Physics of Nuclear Fission. Beijing: Peking University Press, 1999. 133-211
9 Dubray N, Goutte H, Delaroche J P. Phys. Rev. C, 2008, **77**: 014310
10 Younes W, Gogny D. Phys. Rev. C, 2009, **80**: 054313
11 Möller P, Madland D G, Sierk A J et al. Nature, 2001, **409**: 785-790
12 Möller P, Sierk A J, Iwamoto A. Phys. Rev. Lett., 2004, **92**: 072501
13 Möller P, Sierk A J, Ichikawa T et al. Phys. Rev. C, 2009, **79**: 064304
14 Randrup J, Möller P, Sierk A J. Phys. Rev. C, 2011, **84**: 003461
15 Brosa U, Grossmann S, Müller A. Phys. Rep., 1990, **197**: 167-262
16 Duijvestijn M C, Koning A J, Hambsch F J. Phys. Rev. C, 2001, **64**: 014607
17 Koning A J, Hilaire S, Duijvestijn M C. TALYS-1.0. France: EDP Sciences, 2007. 211
18 LIU T J, SUN Z J. Proc. Fission Product Yields: Minor Actinides up to 150 MeV. Ed. Lammer M. Vienna: IAEA, 2008. 323
19 Katakura J. Proc. Fission Product Yields: Minor Actinides up to 150 MeV. Ed. Lammer M. Vienna: IAEA, 2008. 149
20 Wahl A C. Proc. Fission Product Yields: Minor Actinides up to 150 MeV. Ed. Lammer M. Vienna: IAEA, 2008. 117
21 Lammer M. Proc. Fission Product Yields: Minor Actinides up to 150 MeV. Ed. Lammer M. Vienna: IAEA, 2008. 253
22 LIU M, WANG N, LI Z X. Nucl. Phys. A, 2006, **768**: 80–98
23 WANG N, LIU M, YANG Y X. Sci. China Ser. G, 2009, **52**: 1554–1573
24 SUN X J, YU C G, WANG N. Phys. Rev. C, 2012, **85**: 014613
25 Madland D G. Nucl. Phys. A, 2006, **772**: 113–137
26 Shcherbakov O, Donets A, Evdokimov A et al. J. Nucl. Sci. Technol., 2002, **2**(Supplement): 230–233
27 Lisowski P W, Gavron A, Parker W E et al. Fission cross section Ratios for ^{233,234,236}U Relative to ^{235}U from 0.5 10 400 MeV. Berlin: Springer, 1992. 732
28 Lisowski P W, Gavron A, Parker W E et al. Fission Cross Sections in the Intermediate Energy Region. Paris: OECD, 1991. 177
29 Simutkin V. Ph. D. Thesis, Acta Universitatis Upsaliensis, Uppsala, 2011. 35
30 Vivès F, Hambsch F J, Bax H et al. Nucl. Phys. A, 2000, **662**: 63-92
31 Zöller C. Seminar on Fission, Belgium: Pont d'Oye III Habayla-Neuve, 1995. 56